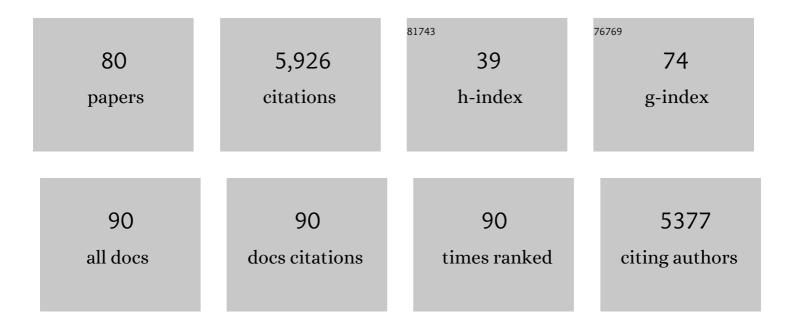
## Malene RingkjÃ, bing Jensen

List of Publications by Year in descending order

Source: https://exaly.com/author-pdf/7381350/publications.pdf Version: 2024-02-01



#	Article	IF	CITATIONS
1	<i>Flexible-meccano:</i> a tool for the generation of explicit ensemble descriptions of intrinsically disordered proteins and their associated experimental observables. Bioinformatics, 2012, 28, 1463-1470.	1.8	324
2	Targeting the disordered C terminus of PTP1B with an allosteric inhibitor. Nature Chemical Biology, 2014, 10, 558-566.	3.9	294
3	NMR Characterization of Long-Range Order in Intrinsically Disordered Proteins. Journal of the American Chemical Society, 2010, 132, 8407-8418.	6.6	276
4	Plasticity of an Ultrafast Interaction between Nucleoporins and Nuclear Transport Receptors. Cell, 2015, 163, 734-745.	13.5	255
5	Exploring Free-Energy Landscapes of Intrinsically Disordered Proteins at Atomic Resolution Using NMR Spectroscopy. Chemical Reviews, 2014, 114, 6632-6660.	23.0	252
6	Describing intrinsically disordered proteins at atomic resolution by NMR. Current Opinion in Structural Biology, 2013, 23, 426-435.	2.6	193
7	Quantitative Description of Backbone Conformational Sampling of Unfolded Proteins at Amino Acid Resolution from NMR Residual Dipolar Couplings. Journal of the American Chemical Society, 2009, 131, 17908-17918.	6.6	187
8	Intrinsic disorder in measles virus nucleocapsids. Proceedings of the National Academy of Sciences of the United States of America, 2011, 108, 9839-9844.	3.3	179
9	Predictive Atomic Resolution Descriptions of Intrinsically Disordered hTau40 and α-Synuclein in Solution from NMR and Small Angle Scattering. Structure, 2014, 22, 238-249.	1.6	171
10	Defining Conformational Ensembles of Intrinsically Disordered and Partially Folded Proteins Directly from Chemical Shifts. Journal of the American Chemical Society, 2010, 132, 1270-1272.	6.6	165
11	A thermodynamic switch modulates abscisic acid receptor sensitivity. EMBO Journal, 2011, 30, 4171-4184.	3.5	161
12	Quantitative Determination of the Conformational Properties of Partially Folded and Intrinsically Disordered Proteins Using NMR Dipolar Couplings. Structure, 2009, 17, 1169-1185.	1.6	160
13	Measles virus nucleo- and phosphoproteins form liquid-like phase-separated compartments that promote nucleocapsid assembly. Science Advances, 2020, 6, eaaz7095.	4.7	148
14	Visualizing the Molecular Recognition Trajectory of an Intrinsically Disordered Protein Using Multinuclear Relaxation Dispersion NMR. Journal of the American Chemical Society, 2015, 137, 1220-1229.	6.6	128
15	Quantitative Conformational Analysis of Partially Folded Proteins from Residual Dipolar Couplings: Application to the Molecular Recognition Element of Sendai Virus Nucleoprotein. Journal of the American Chemical Society, 2008, 130, 8055-8061.	6.6	127
16	Structure of Nipah virus unassembled nucleoprotein in complex with its viral chaperone. Nature Structural and Molecular Biology, 2014, 21, 754-759.	3.6	119
17	Binding Mechanisms of Intrinsically Disordered Proteins: Theory, Simulation, and Experiment. Frontiers in Molecular Biosciences, 2016, 3, 52.	1.6	118
18	Mapping the Potential Energy Landscape of Intrinsically Disordered Proteins at Amino Acid Resolution. Journal of the American Chemical Society, 2012, 134, 15138-15148.	6.6	113

#	Article	IF	CITATIONS
19	Structure of the Vesicular Stomatitis Virus NO-P Complex. PLoS Pathogens, 2011, 7, e1002248.	2.1	111
20	Structural characterization of αâ€ <b>s</b> ynuclein in an aggregation prone state. Protein Science, 2009, 18, 1840-1846.	3.1	97
21	Towards a robust description of intrinsic protein disorder using nuclear magnetic resonance spectroscopy. Molecular BioSystems, 2012, 8, 58-68.	2.9	95
22	PED in 2021: a major update of the protein ensemble database for intrinsically disordered proteins. Nucleic Acids Research, 2021, 49, D404-D411.	6.5	95
23	Identification of Dynamic Modes in an Intrinsically Disordered Protein Using Temperature-Dependent NMR Relaxation. Journal of the American Chemical Society, 2016, 138, 6240-6251.	6.6	90
24	Solution structure of the Câ€ŧerminal X domain of the measles virus phosphoprotein and interaction with the intrinsically disordered Câ€ŧerminal domain of the nucleoprotein. Journal of Molecular Recognition, 2010, 23, 435-447.	1.1	81
25	Elucidating binding mechanisms and dynamics of intrinsically disordered protein complexes using NMR spectroscopy. Current Opinion in Structural Biology, 2019, 54, 10-18.	2.6	78
26	Conformational Propensities of Intrinsically Disordered Proteins from NMR Chemical Shifts. ChemPhysChem, 2013, 14, 3034-3045.	1.0	69
27	Atomic Resolution Description of the Interaction between the Nucleoprotein and Phosphoprotein of Hendra Virus. PLoS Pathogens, 2013, 9, e1003631.	2.1	68
28	Characterization of intrinsically disordered proteins and their dynamic complexes: From in vitro to cell-like environments. Progress in Nuclear Magnetic Resonance Spectroscopy, 2018, 109, 79-100.	3.9	67
29	Structure of the Tetramerization Domain of Measles Virus Phosphoprotein. Journal of Virology, 2013, 87, 7166-7169.	1.5	66
30	Characterization of the Interactions between the Nucleoprotein and the Phosphoprotein of Henipavirus. Journal of Biological Chemistry, 2011, 286, 13583-13602.	1.6	65
31	Structure and dynamics of the MKK7–JNK signaling complex. Proceedings of the National Academy of Sciences of the United States of America, 2015, 112, 3409-3414.	3.3	64
32	Deciphering the Dynamic Interaction Profile of an Intrinsically Disordered Protein by NMR Exchange Spectroscopy. Journal of the American Chemical Society, 2018, 140, 1148-1158.	6.6	64
33	Self-association of a highly charged arginine-rich cell-penetrating peptide. Proceedings of the National Academy of Sciences of the United States of America, 2017, 114, 11428-11433.	3.3	63
34	Small-Angle X-Ray Scattering- and Nuclear Magnetic Resonance-Derived Conformational Ensemble of the Highly Flexible Antitoxin PaaA2. Structure, 2014, 22, 854-865.	1.6	61
35	A Unified Description of Intrinsically Disordered Protein Dynamics under Physiological Conditions Using NMR Spectroscopy. Journal of the American Chemical Society, 2019, 141, 17817-17829.	6.6	55
36	NMR Provides Unique Insight into the Functional Dynamics and Interactions of Intrinsically Disordered Proteins. Chemical Reviews, 2022, 122, 9331-9356.	23.0	51

#	Article	IF	CITATIONS
37	The intrinsically disordered SARS-CoV-2 nucleoprotein in dynamic complex with its viral partner nsp3a. Science Advances, 2022, 8, eabm4034.	4.7	50
38	The N <sup>0</sup> â€binding region of the vesicular stomatitis virus phosphoprotein is globally disordered but contains transient αâ€helices. Protein Science, 2011, 20, 542-556.	3.1	49
39	Large-Scale Conformational Dynamics Control H5N1 Influenza Polymerase PB2 Binding to Importin α. Journal of the American Chemical Society, 2015, 137, 15122-15134.	6.6	49
40	An ultraweak interaction in the intrinsically disordered replication machinery is essential for measles virus function. Science Advances, 2018, 4, eaat7778.	4.7	49
41	Accurate characterization of weak macromolecular interactions by titration of NMR residual dipolar couplings: application to the CD2AP SH3-C:ubiquitin complex. Nucleic Acids Research, 2009, 37, e70-e70.	6.5	46
42	Modulation of the Intrinsic Helix Propensity of an Intrinsically Disordered Protein Reveals Long-Range Helix–Helix Interactions. Journal of the American Chemical Society, 2013, 135, 10155-10163.	6.6	44
43	Molecular basis of host-adaptation interactions between influenza virus polymerase PB2 subunit and ANP32A. Nature Communications, 2020, 11, 3656.	5.8	43
44	Specific and Nonspecific Interactions in Ultraweak Protein–Protein Associations Revealed by Solvent Paramagnetic Relaxation Enhancements. Journal of the American Chemical Society, 2014, 136, 10277-10286.	6.6	41
45	Selfâ€Assembly of Measles Virus Nucleocapsidâ€like Particles: Kinetics and RNA Sequence Dependence. Angewandte Chemie - International Edition, 2016, 55, 9356-9360.	7.2	41
46	Sequence-Specific Mapping of the Interaction between Urea and Unfolded Ubiquitin from Ensemble Analysis of NMR and Small Angle Scattering Data. Journal of the American Chemical Society, 2012, 134, 4429-4436.	6.6	38
47	Pilotin–secretin recognition in the type II secretion system of <i>Klebsiella oxytoca</i> . Molecular Microbiology, 2011, 82, 1422-1432.	1.2	37
48	Ensemble Structure of the Modular and Flexible Full-Length Vesicular Stomatitis Virus Phosphoprotein. Journal of Molecular Biology, 2012, 423, 182-197.	2.0	37
49	Probing electric fields in proteins in solution by NMR spectroscopy. Proteins: Structure, Function and Bioinformatics, 2008, 72, 333-343.	1.5	36
50	Quantitative Modelfree Analysis of Urea Binding to Unfolded Ubiquitin Using a Combination of Small Angle X-ray and Neutron Scattering. Journal of the American Chemical Society, 2009, 131, 8769-8771.	6.6	36
51	Structure, dynamics and phase separation of measles virus RNA replication machinery. Current Opinion in Virology, 2020, 41, 59-67.	2.6	36
52	Assembly and cryo-EM structures of RNA-specific measles virus nucleocapsids provide mechanistic insight into paramyxoviral replication. Proceedings of the National Academy of Sciences of the United States of America, 2019, 116, 4256-4264.	3.3	35
53	On the Origin of NMR Dipolar Waves in Transient Helical Elements of Partially Folded Proteins. Journal of the American Chemical Society, 2008, 130, 11266-11267.	6.6	33
54	Multiâ€Timescale Conformational Dynamics of the SH3 Domain of CD2â€Associated Protein using NMR Spectroscopy and Accelerated Molecular Dynamics. Angewandte Chemie - International Edition, 2012, 51, 6103-6106.	7.2	33

#	Article	IF	CITATIONS
55	Structural and Biophysical Characterization of Murine Rif1 C Terminus Reveals High Specificity for DNA Cruciform Structures. Journal of Biological Chemistry, 2014, 289, 13903-13911.	1.6	32
56	Insights into the Structure and Dynamics of Measles Virus Nucleocapsids by 1H-detected Solid-state NMR. Biophysical Journal, 2014, 107, 941-946.	0.2	30
57	Quantitative Description of Intrinsically Disordered Proteins Using Single-Molecule FRET, NMR, and SAXS. Journal of the American Chemical Society, 2021, 143, 20109-20121.	6.6	29
58	Structural Description of the Nipah Virus Phosphoprotein and Its Interaction with STAT1. Biophysical Journal, 2020, 118, 2470-2488.	0.2	28
59	Testing the validity of ensemble descriptions of intrinsically disordered proteins. Proceedings of the National Academy of Sciences of the United States of America, 2014, 111, E1557-8.	3.3	27
60	Binding ability of a HHP-tagged protein towards Ni2+studied by paramagnetic NMR relaxation: The possibility of obtaining long-range structure information. Journal of Biomolecular NMR, 2004, 29, 175-185.	1.6	26
61	Visualizing protein breathing motions associated with aromatic ring flipping. Nature, 2022, 602, 695-700.	13.7	26
62	Structural Disorder within Sendai Virus Nucleoprotein and Phosphoprotein: Insight into the Structural Basis of Molecular Recognition. Protein and Peptide Letters, 2010, 17, 952-960.	0.4	25
63	Intrinsically disordered proteins implicated in paramyxoviral replication machinery. Current Opinion in Virology, 2014, 5, 72-81.	2.6	23
64	Investigating the Role of Large-Scale Domain Dynamics in Protein-Protein Interactions. Frontiers in Molecular Biosciences, 2016, 3, 54.	1.6	23
65	A General Method for Determining the Electron Self-Exchange Rates of Blue Copper Proteins by Longitudinal NMR Relaxation. Journal of the American Chemical Society, 2002, 124, 4093-4096.	6.6	22
66	Disentangling the Coil: Modulation of Conformational and Dynamic Properties by Site-Directed Mutation in the Non-Native State of Hen Egg White Lysozyme. Biochemistry, 2012, 51, 3361-3372.	1.2	22
67	Direct Prediction of NMR Residual Dipolar Couplings from the Primary Sequence of Unfolded Proteins. Angewandte Chemie - International Edition, 2013, 52, 687-690.	7.2	19
68	Exploring the Minimally Frustrated Energy Landscape of Unfolded ACBP. Journal of Molecular Biology, 2014, 426, 722-734.	2.0	17
69	Distinct Ubiquitin Binding Modes Exhibited by SH3 Domains: Molecular Determinants and Functional Implications. PLoS ONE, 2013, 8, e73018.	1.1	17
70	Ensemble Structure of the Highly Flexible Complex Formed between Vesicular Stomatitis Virus Unassembled Nucleoprotein and its Phosphoprotein Chaperone. Journal of Molecular Biology, 2016, 428, 2671-2694.	2.0	16
71	Quantitative Conformational Analysis of Functionally Important Electrostatic Interactions in the Intrinsically Disordered Region of Delta Subunit of Bacterial RNA Polymerase. Journal of the American Chemical Society, 2019, 141, 16817-16828.	6.6	16
72	A Combined NMR and SAXS Analysis of the Partially Folded Cataract-Associated V75D γD-Crystallin. Biophysical Journal, 2017, 112, 1135-1146.	0.2	15

#	Article	IF	CITATIONS
73	Functionally specific binding regions of microtubule-associated protein 2c exhibit distinct conformations and dynamics. Journal of Biological Chemistry, 2018, 293, 13297-13309.	1.6	13
74	Weak selfâ€association of human growth hormone investigated by nitrogenâ€15 NMR relaxation. Proteins: Structure, Function and Bioinformatics, 2008, 73, 161-172.	1.5	12
75	Characterizing weak protein–protein complexes by NMR residual dipolar couplings. European Biophysics Journal, 2011, 40, 1371-1381.	1.2	10
76	Revealing the mechanism of repressor inactivation during switching of a temperate bacteriophage. Proceedings of the National Academy of Sciences of the United States of America, 2020, 117, 20576-20585.	3.3	6
77	Structural basis of the bacteriophage <scp>TP</scp> 901â€l <scp>CI</scp> repressor dimerization and interaction with <scp>DNA</scp> . FEBS Letters, 2018, 592, 1738-1750.	1.3	5
78	Enthalpy–Entropy Compensation in the Promiscuous Interaction of an Intrinsically Disordered Protein with Homologous Protein Partners. Biomolecules, 2021, 11, 1204.	1.8	5
79	Experimental studies of binding of intrinsically disordered proteins to their partners. , 2019, , 139-187.		3
80	Inside Back Cover: Multi-Timescale Conformational Dynamics of the SH3 Domain of CD2-Associated Protein using NMR Spectroscopy and Accelerated Molecular Dynamics (Angew. Chem. Int. Ed. 25/2012). Angewandte Chemie - International Edition, 2012, 51, 6279-6279.	7.2	0